Eur Biophys J (1987) 14: 359–368

European Biophysics Journal

Analysis of ligand-binding to the kringle 4 fragment from human plasminogen

A. De Marco[1]*, A. M. Petros[1], R. A. Laursen[2], and M. Llinás[1]

[1] Department of Chemistry, Carnegie-Mellon University, Pittsburgh, PA 15213, USA
[2] Department of Chemistry, Boston University, Boston, MA 02215, USA

Received June 30, 1986/Accepted in revised form October 2, 1986

Abstract. The interaction of the isolated human plasminogen kringle 4 with the four ω-amino acid ligands ε-aminocaproic acid (εACA), N^{α}-acetyl-L-lysine (AcLys), *trans*-aminomethyl(cyclohexane)carboxylic acid (AMCHA) and *p*-benzylaminesulfonic acid (BASA) has been further characterized by ^{1}H-NMR spectroscopy at 300 and 600 MHz. Pronounced high-field shifts, reaching ~ 3 ppm, are observed for AMCHA resonances upon binding to kringle 4, which underscores the relevance of ligand lipophilic interactions with aromatic side chains at the binding site. Ligand titration curves for the nine His and Trp singlets found in the kringle 4 aromatic spectrum reveal a striking uniformity in the kringle response to the various ligands. The average binding curves exhibit a clear Langmuir absorption isotherm saturation profile and the data were analyzed under the assumption of one (high affinity) binding site per kringle. Equilibrium association constants (K_a) and first order dissociation rate constants (k_{off}) were derived from linearized expressions of the Langmuir isotherm and of the spectral line-shapes, respectively. The results for the four ligands, at ~ 295 K, pH* 7.2, indicate that: (a) AMCHA exhibits the strongest binding ($K_a = 159\ mM^{-1}$) and εACA the weakest ($K_a = 21\ mM^{-1}$) with AcLys and BASA falling in between; (b) εACA dissociates readily ($k_{off} = 5.3 \times 10^3\ s^{-1}$) and AMCHA associates the fastest ($k_{on} = 2.0 \times 10^8\ M^{-1}\ s^{-1}$) while the kinetics for BASA exchange is relatively slow ($k_{off} = 0.8 \times 10^3\ s^{-1}$, $k_{on} = 0.6 \times 10^8\ M^{-1}\ s^{-1}$); (c) the ligand-binding kinetics is close to diffussion-controlled.

Key words: Antifibrinolytics, kringle 4 association constants, kringle 4 ligand kinetics, lysine-binding site, plasminogen NMR

Introduction

Of the five kringle domains found in human plasminogen (Sottrup-Jensen et al. 1978) kringles 1 and 4 are known to bind lysine and related ω-amino acids (Sottrup-Jensen et al. 1978; Lerch et al. 1980; Winn et al. 1980; Markus et al. 1981; De Marco et al. 1982; Váli and Patthy 1982). Although the physiological role of the lysine-binding site is not clear (Thorsen et al. 1981; Váli and Patthy 1984), an increasing body of evidence suggests that it might interact with α_2-antiplasmin and, most importantly, afford a mechanism for anchoring plasmin(ogen) to fibrin and fibrin clots (Wiman and Collen 1978; Lucas et al. 1983; Christensen 1984; Bok and Mangel 1985). Furthermore, the interaction of plasminogen kringles with lysine and ω-amino acid analogs of lysine provides the basis for the selective extraction of plasminogen from blood plasma and for the purification of the isolated kringles 1 and 4 proteolytic fragments via affinity chromatography on lysine-conjugated support gels (Deutsch and Mertz 1970; Sottrup-Jensen et al. 1978; Lerch et al. 1980). It is interesting that many of these ω-amino acids exhibit potent antifibrinolytic activity to the extent that some of them are clinically exploited to control fibrinolysis (Markwardt 1978).

Recently, we have reported on the ^{1}H-NMR spectroscopic aspects of ligand-binding to kringle 4 (Llinás et al. 1985; De Marco et al. 1986). Of the four investigated ligands, εACA, AcLys, AMCHA and BASA (Scheme I), the first two are linear

* Permanent address: Istituto di Chimica delle Macromolecole, Consiglio Nazionale delle Ricerche, Via E. Bassini 15/A, I-20133 Milano, Italy

Abbreviations: εACA, ε-aminocaproic acid; AcLys, N^{α}-acetyl-L-lysine, AMCHA, *t*-aminomethyl(cyclohexane)carboxylic acid; BASA, *p*-benzylaminesulfonic acid; K4, kringle 4; NOE, nuclear Overhauser effect; ppm, parts-per-million; pH*, glass electrode pH reading uncorrected for deuterium isotope effects; K_a, ligand-kringle 4 equilibrium association constant; k_{off}, ligand-kringle 4 dissociation rate constant; k_{on}, ligand-kringle 4 association rate constant

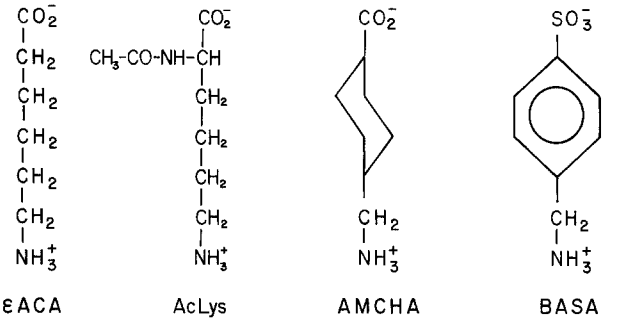

Scheme I: Ligand structures

molecules and the latter two contain 6-member ring structures, BASA being aromatic while AMCHA is not. The four ligands are zwitterionic, exhibiting a dipolar distance of $\gtrsim 6.8$ Å which has been shown to be about optimal in terms of stabilizing the kringle-ligand interaction (Okamoto et al. 1968; Markwardt 1978; Winn et al. 1980). In these NMR studies our main concern has been to analyze the spectroscopic information in terms of the structure of the ligand-binding site (Llinás et al. 1985; De Marco et al. 1986). Here, our primary objective is to quantitate the ligand titration data in order to derive values for the ligand-kringle 4 association constants (K_a) and for the kinetic parameters (k_{on}, k_{off}) which characterize the association-dissociation complexation reactions. For the former purpose we have monitored the positions of the nine His + Trp singlets in the aromatic spectrum of kringle 4 (Llinás et al. 1983; Trexler et al. 1983; De Marco et al. 1985b) as well as the chemical shifts of other conveniently resolved kringle resonances. The singlets afford relatively narrow signals which can be followed readily in the course of ligand titration experiments. Ligand-binding rate constants can, in turn, be derived from line-shape analyses of selected resonances (Sudmeier et al. 1980). It is fortunate that the spectral perturbations, mainly line broadenings and chemical shifts, induced by diamagnetic ligands on the kringles and, reciprocally, caused by the kringles on the ligands, can be analyzed in terms of equilibrium and kinetic parameters quite independently of a detailed characterization of their corresponding spectra.

Materials and methods

Kringle 4 was isolated from human plasminogen by elastase digestion of the zymogen (Sottrup-Jensen et al. 1978) as described elsewhere (Winn et al. 1980). The ^{1}H-NMR spectra of kringle 4 were recorded in the Fourier mode at 300 MHz with a Bruker WM-300 spectrometer or at 600 MHz using the National NMR Facility for Biomedical Research at Carnegie-Mellon University. The experiments were performed at $\sim 22\,^\circ$C, pH* 7.2, for the protein sample dissolved in ^2H_2O. The kringle was pre-exchanged against ^2H_2O to eliminate signals arising from exchangeable protons. Ligand titration was implemented by adding measured amounts of concentrated ligand, dissolved in ^2H_2O, to the NMR tube containing the kringle sample. The volumes of the ligand additions were controlled with a micrometer syringe. Typically 2–5 µl were added at once to 0.4 ml of $10^{-3}\,M$ kringle 4 solution contained in a 5 mm NMR tube. Dioxane was used as internal reference frequency standard; chemical shifts are referred to the sodium 3-trimethylsilyl(2,2,3,3-$^2H_4$)-propionate signal (De Marco 1977). pH* was measured before and after each titration experiment to check for any acid/base drift. Spectral simulations, implemented to derive reasonable resonance line width values, were accomplished using the PANIC Program (Bruker Aspect 2000 Data Package).

Results

Figure 1A shows the high-field, methyl region ^{1}H-NMR spectrum of kringle 4 at 300 MHz. Most noticeable markers are doublets 1 and 2 which arise from the Leu^{46} side chain $CH_3^{\delta,\delta'}$ groups, and the unresolved resonances 3 and 4 assigned to Leu^{77} (Llinás et al. 1983). These doublets are broad and shifted to high-field relative to their "random coil" positions at ~ 0.9 ppm (Bundi and Wüthrich 1979). These characteristics reflect a significant loss of side chain motional freedom and close interaction of the methyl groups with internal aromatic rings as shown by efficient cross-relaxation (Overhauser) effects (De Marco et al. 1985a). Other relatively sharper methyl signals appear at $\delta > 0.5$ ppm; these have been analyzed elsewhere (Llinás et al. 1983). It is observed that addition of ω-amino acid ligands perturbs only minimally the methyl spectrum (Llinás et al. 1985; De Marco et al. 1986). Most noteworthy are an overall sharpening of resonances and a small, but measurable, shift of the Leu^{46} $CH_3^{\delta,\delta'}$ signals. The decrease in line widths is most likely caused by ligand interference with kringle self-aggregation (Ramesh et al. 1986) while the shifts induced on the Leu^{46} methyl doublets, observed for all ligands we have studied to-date, appear to arise indirectly, from a perturbation of the aromatic rings which are in contact with the Leu^{46} side chain. Figure 1B illustrates these effects for the ligand AMCHA. The appearance of broad "humps" at ~ 1.1 and ~ 1.35 ppm reflects the contribution of two AMCHA equatorial proton multiplets shown in Spectrum C for the free ligand, which are broadened when in presence

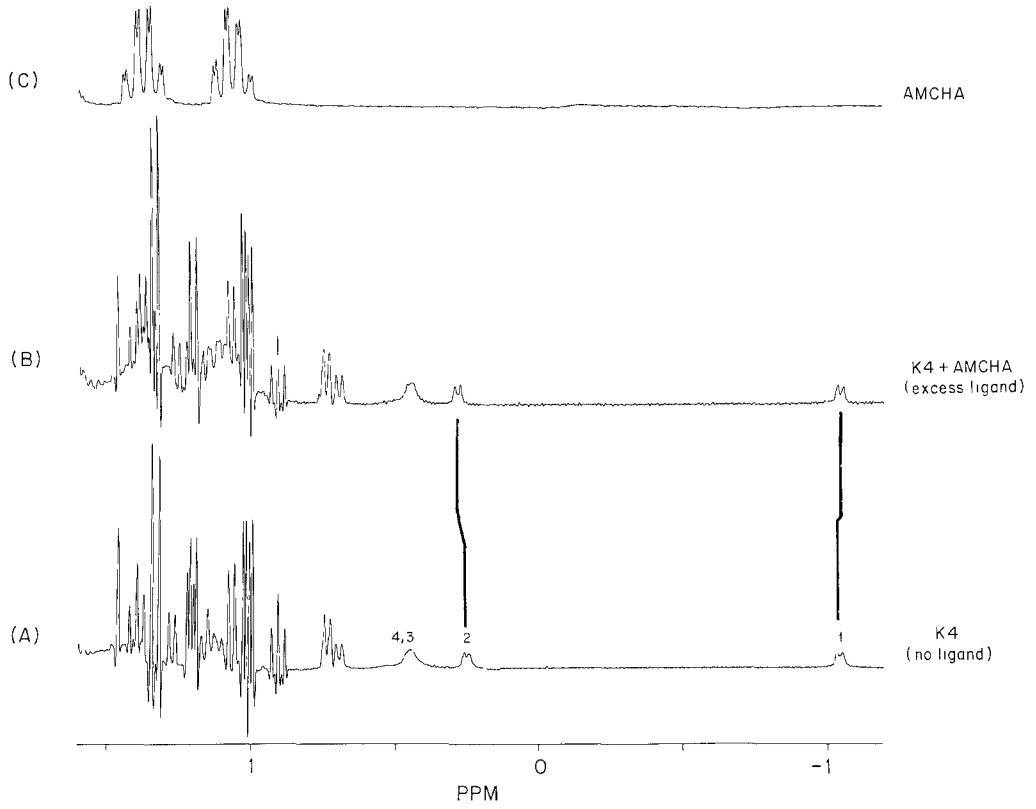

Fig. 1 A–C. Effect of AMCHA-binding on the 300 MHz ^{1}H-NMR methyl spectrum of kringle 4 from human plasminogen. **A** High-field spectrum of kringle 4, no ligand. **B** Same as (**A**), but in presence of excess AMCHA; ligand-induced shifts of the Leu^{46} $CH_3^{\delta,\delta'}$ resonances 1 and 2 are indicated. **C** Partial spectrum of AMCHA, whose resonances (broadened) also contribute to spectrum (**B**). Kringle 4 concentration ~ 1 m*M*, pH* 7.2, 298 K. Spectra (**A**) and (**B**) are resolution enhanced

of kringle 4 because of fast (bound $\rightleftharpoons$ free) exchange.

It is to be expected that at substoichiometric ligand levels, i.e. when most ligand is bound, signals from the latter ought to exhibit the spectral characteristics of its kringle-bound state as fixed by the protein environment. That this is the case is shown by Fig. 2, which depicts expanded the $-2.2 < \delta < 0.2$ ppm kringle 4 spectral region in the absence of ligand (Spectrum A) and with increasing levels of added AMCHA (Spectra B–F). A set of five broad resonances, labelled a–e, are seen to appear upon minimal ligand additions. These arise from AMCHA protons since they increase in intensity as ligand is added (spectra A–D) to eventually broaden and shift downfield (Spectra E, F) to appear, for excess ligand, at the free AMCHA spectral positions (Fig. 1B and C). This behavior is typical of rapid ligand exchange between free and bound states (Sudmeier et al. 1980). Integration of resonances a, b and e (Fig. 2), normalized to the area of the Leu^{46} CH_3^{δ} resonance at ~ -1 ppm, shows that each of these signals arises from a single proton on the AMCHA molecule while the overlapping c + d signal stems from exactly two such protons. Most noteworthy in Fig. 2 are the exaggerated high-field shifts of the bound AMCHA signals which can only arise from ring-current effects and thus afford unique evidence for direct ligand-aromatic side chain interactions at the kringle's lysine-binding site. Furthermore, the rather well defined appearance of the AMCHA signals at [ligand]/[kringle] levels as high as ~ 0.78:1 suggests a relatively tight binding of the drug. It should be indicated that in a previous study (De Marco et al. 1986) signal a in Fig. 2C was not observed because the spectrum, recorded in the "fast scan" correlation mode, was not swept far enough to high-field as a ligand resonance at ~ -2 ppm was unforeseen.

The complete aromatic ^{1}H-NMR spectrum of kringle 4 has been reported and analyzed elsewhere (De Marco et al. 1985b; Ramesh et al. 1986). As discussed in previous papers (Llinás et al. 1985; De Marco et al. 1986), it is this spectral region which is the most sensitive to ligand-binding. For the purposes of this investigation we chose to monitor, among others, the ligand response of nine aromatic singlets assigned as follows: (a) singlets 1, 4 and 7, which correspond to the indole H2 protons of Trp^{72}, Trp-I (Trp^{25}?) and Trp-II (Trp^{62}?), respectively; (b)

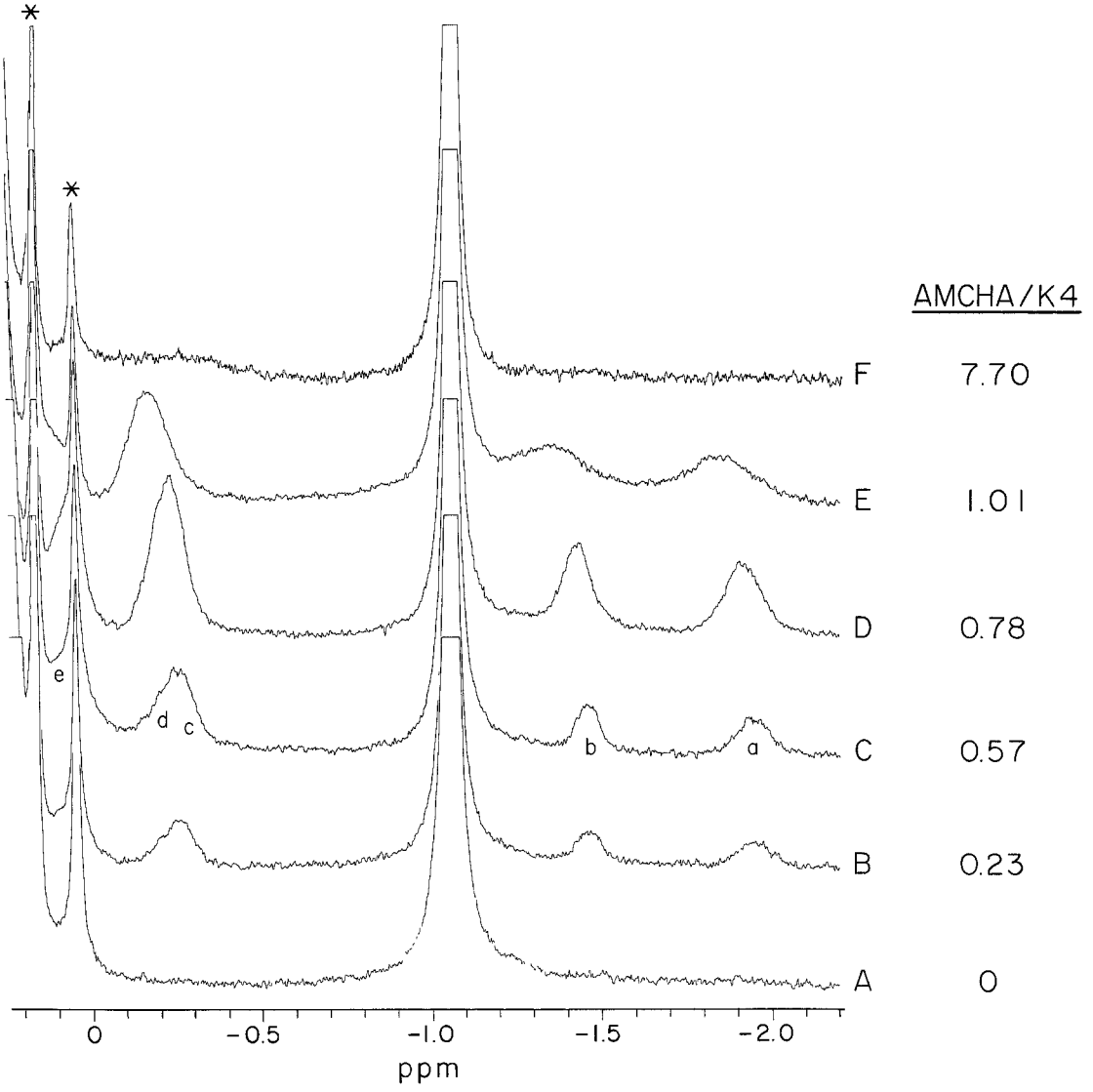

Fig. 2A–F. Expansion of the 300 MHz high-field spectrum of kringle 4 in the presence of variable amounts of AMCHA. The large resonances at ~ -1.05 ppm and at $\delta > 0.1$ ppm arise from the Leu^{46} $CH_3^{\delta,\delta'}$ doublets. Resonances stemming from bound ligand are labelled $a-e$. Impurities in the sample are indicated (*). **A** Control spectrum, no ligand; **B–F** spectra recorded in the presence of increasing concentrations of AMCHA; the AMCHA/K4 molar ratio is indicated on the right. Kringle 4 concentration ~ 1 m*M*, pH* 7.2, 295 K

singlet pairs 2 + 8, 3 + 6 and 9 + 5, which correspond to the imidazole H4+H2 protons of His^{33}, His^{3} and His^{31}, respectively (Ramesh et al. 1986). In the case of kringle 1, we have reported complete BASA titration curves of the corresponding singlets which enabled us to derive an estimate of the ligand-kringle association constant K_a (De Marco et al. 1982). Figures 3–6 show similar curves for kringle 4, where εACA, AcLys, AMCHA and BASA are the ligands. The curves result from plotting $\Delta\delta$, the singlet chemical shift after ligand addition referred to that in the free kringle, versus $[S_0]/[K_0]$, the concentration ratio between the total added ligand and the total (free + bound) kringle, the latter determined from optimal fittings (see Discussion).

The Trp^{72} singlet 1 undergoes only minor shifts when in presence of the linear ligands, being essentially unperturbed by AcLys (Fig. 4). At 600 MHz it is observed to strongly broaden after a first, substoichiometric addition of εACA, to eventually reappear (close to its initial position) when in the presence of a large excess of ligand (Fig. 3). Such behavior is not apparent at 300 MHz, suggesting that the broadening results from a ligand exchange process that matches the observational frequency at 600 MHz but is fast on the 300 MHz time scale. Shifted to higher fields by AMCHA (Fig. 5), singlet 1 is dramatically affected by BASA, strongly shifting, broadening to the extent of becoming nondetectable, then reappearing and sharpening pro-

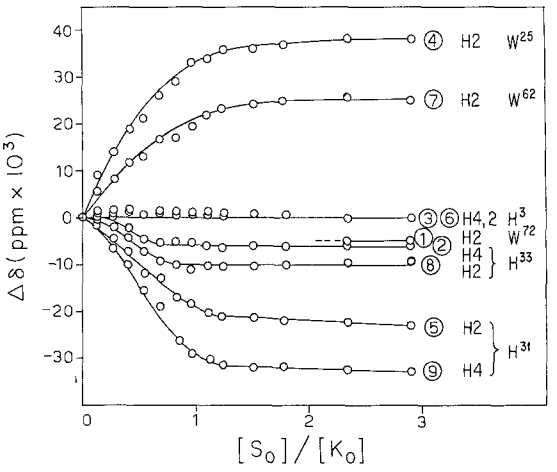

Fig. 3. Binding εACA to kringle 4: ligand titration curves for His and Trp aromatic singlets. Singlets are numbered as in a previous paper (De Marco et al. 1985b). Trp indole H2 resonances: singlets 1 (W-III = Trp^{72}), 4 (W-I = Trp^{25} or Trp^{62}), and 7 (W-II = Trp^{62} or Trp^{25}). His imidazole H2+H4 resonances: singlets 8+2 (H-III = His^{33}), 6+3 (H-I = His^{3}), and 5+9 (H-II = His^{31}). Data extracted from spectra recorded at 600 MHz, pH* 7.2, 25 °C, $\Delta\delta$, chemical shift of a singlet relative to its chemical shift in the absence of ligand; $[S_0]/[K_0]$, concentration ratio of total added ligand to total (free + bound) kringle 4

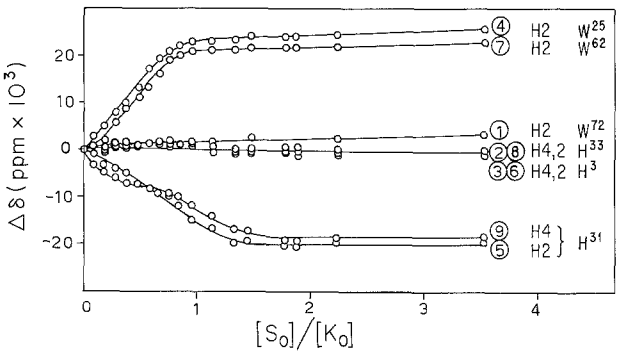

Fig. 4. Binding of AcLys to kringle 4: ligand titration curves for His and Trp aromatic singlets. Experimental conditions and meaning of labels are given in the caption to Fig. 3

gressively to eventually consolidate itself at ~ 0.4 ppm to higher fields (off-scale in Fig. 6). The above evidence indicates, once more, that when the kringle is in the presence of near stoichiometric levels of BASA, the Trp^{72} singlet exchange between bound and unbound states is neither fast nor slow but intermediate on the 600 MHz NMR time scale (Feeney et al. 1979; Hochschwender et al. 1983).

As a common feature of the tested ligands, the His^{3} singlets 3 + 6 are minimally perturbed by ligand-binding. This is consistent with the interpretation that the His^{3} side chain, carrying a freely mobile imidazole ring, is removed from the binding site (De Marco et al. 1986). The His^{31} singlets 5 + 9

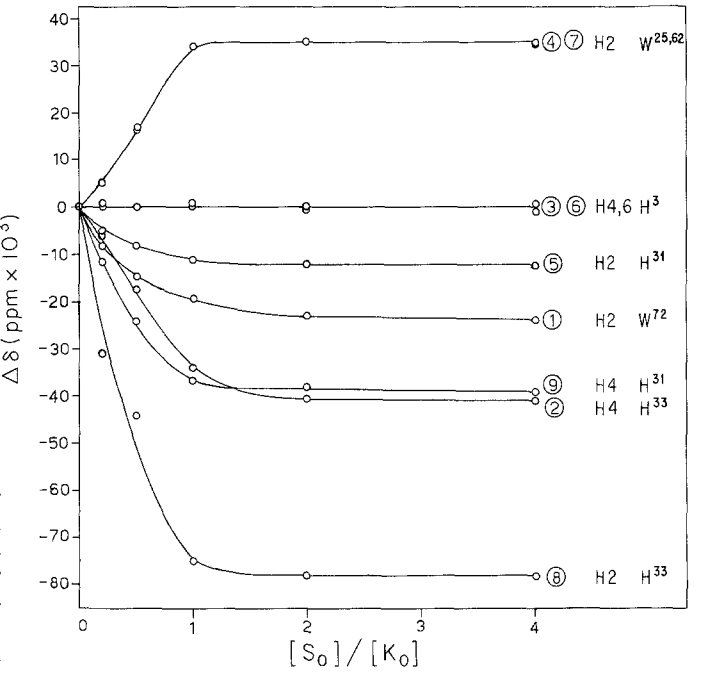

Fig. 5. Binding of AMCHA to kringle 4: ligand titration curves for His and Trp aromatic singlets. Experimental conditions and meaning of labels are given in the caption to Fig. 3

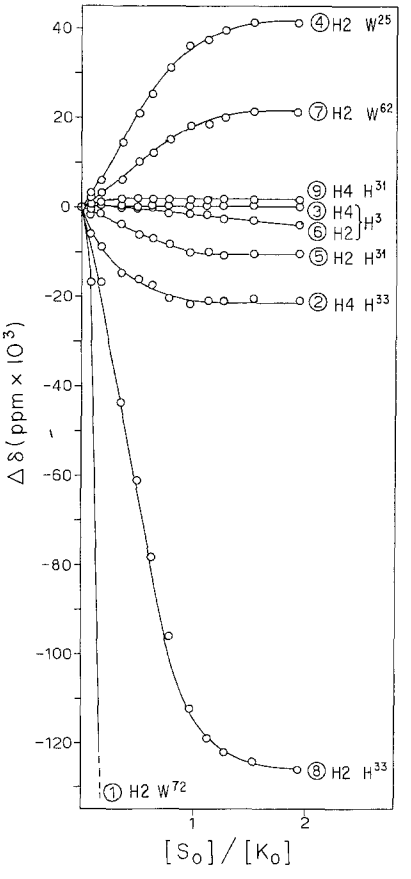

Fig. 6. Binding of BASA to kringle 4: ligand titration curves for His and Trp aromatic singlets. Experimental conditions and meaning of labels are given in the caption to Fig. 3

Table 1. Ligand-induced shifts on kringle 4 aromatic singlets[a]

Singlet	1	2	3	4	5	6	7	8	9
Residue	W^{72}	H^{33}	H^{3}	W^{25}	H^{31}	H^{3}	W^{62}	H^{33}	H^{31}
Proton	H2	H4	H4	H2	H2	H2	H2	H2	H4
εACA	~ −5[b]	−6	0	+38	−23	0	+26	−10	−34
AcLys	0	0	0	+26	−20	0	+23	0	−20
AMCHA	−23	−41	0	+34	−12	0	+34	−78	−39
BASA	−410	−21	0	+41	−10	0	+21	−130	2

[a] Shifts ($\Delta\delta \times 10^3$ ppm) are for kringle 4 in presence of excess ligand and are referred to the singlet frequency in absence of the ligand; low field shifts are positive

[b] Singlet broadens upon substoichiometric ligand additions (see text)

move to higher fields with all ligands except BASA, in which case singlet 5 shifts but 9 does not, a result that is likely to arise from a ring current effect induced by the BASA molecule which opposes the intrinsic ligand perturbation. His^{33} singlets 2 + 8 are also shifted to higher fields by all ligands except AcLys, which indicates, as is the case for His^{31}, that His^{33} is near the binding state.

It is noteworthy that AcLys perturbs *only* Trp^{25}, Trp^{62} and His^{31} thus appearing, from this standpoint, to be the most selective of the investigated ligands (Fig. 4). The latter would suggest that, despite the presence of the acetamide substituent at the C^{α} position, AcLys "fits" the binding site better than does εACA, a structurally simpler compound. Significantly, among the four investigated effectors AcLys represents the closest analog to the putative "natural" ligand: a polypeptide chain segment incorporating L-Lys at the C-terminus (Christensen 1984; Bok and Mangel 1985).

A summary of ligand-binding effects on the His and Trp singlets is given in Table 1. A pattern is evident: on comparing the effects from the various ligands we observe a predominant retention of sign for the ligand-induced chemical shifts, which suggests that the induced shifts mainly reflect local conformational rearrangement of aromatic side chains. In the case of BASA, the large shift of the Trp^{72} singlet 1 points to a direct interaction between the indole group and the ligand ring, as also indicated by BASA-kringle 4 saturation transfer (Overhauser) experiments (Llinás et al. 1985). Furthermore, from inspection of Figs. 3–6 it is clear that all the investigated ligands perturb Trp^{25}, Trp^{62} and His^{31} to various extents. In conjunction with the results from the BASA-kringle 4 saturation transfer experiments (Llinás et al. 1985), this pattern reinforces a model by which the three residues are either at the binding site or positioned very close to it.

Discussion

In the analysis of the ligand-binding data we assume, for simplicity, (a) a single binding site, as established by Lerch et al. (1980) and by Markus et al. (1981), respectively for εACA- and AMCHA-binding to kringle 4; (b) a single association-dissociation mechanism. Furthermore, we use an average titration curve for each ligand, representing the combined response of a number of ligand-sensitive kringle 4 resonances, a device by which measurement errors and deviations from hyperbolic profiles tend to cancel out. The latter are likely to arise from kringle self-aggregation interference with ligand-binding (Hochschwender et al. 1983; Llinás et al. 1983) and/or uncharacterized, weak non-specific binding.

Equilibrium association constants

We assume a two-state system at equilibrium

$$A + X \underset{k_{off}}{\overset{k_{on}}{\rightleftarrows}} B. \qquad (1)$$

If one chooses to monitor kringle resonances, X represents the free ligand while A and B stand for the protein in the free and in the complexed states, respectively. The kringle-ligand association constant $K_a = k_{on}/k_{off}$, is calcualated assuming fast exchange-averaging of the various resonances. This assumption is justified for most of the kringle signals, as shown under Results and discussed elsewhere (De Marco et al. 1986). For our calculations, we have selected data extracted from signals that satisfy this criterion. The chemical shift dependence on populations, measured by the experimental normalized parameter Δ_P (population of the complex) is given by

$$\Delta_P \equiv (\delta_P - \delta_P^Q)/(\delta_P^C - \delta_P^Q) = [KS]/[K_0], \qquad (2)$$

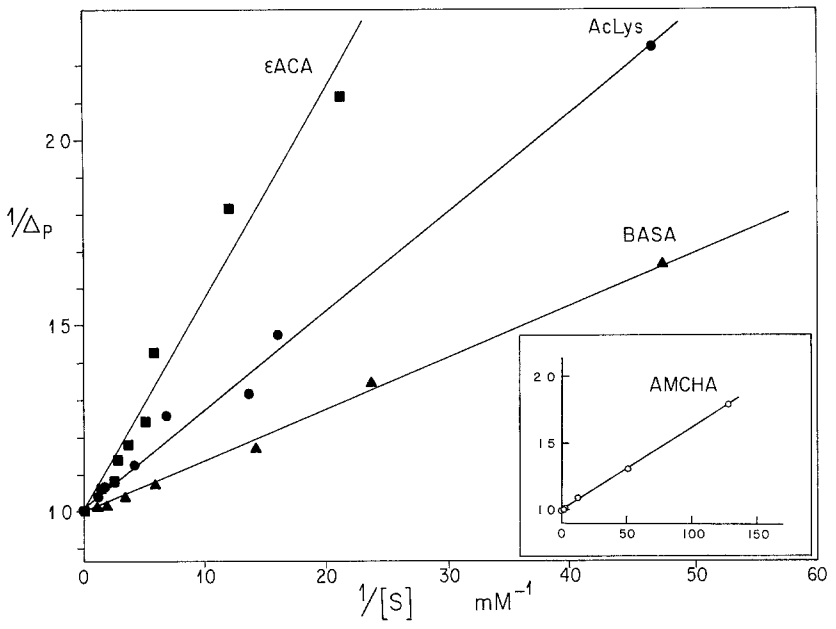

Fig. 7. Linear fittings of ligand titration data for kringle 4. Δ_P values were averaged on various resonances: AcLys (●), εACA (■) and BASA (▲). The data for AMCHA is given in the inset (○). Straight lines result from a linear fitting to Eq. (3) where $[S] = ([S_0] - [K_0]\,\Delta_P)$ corr

where δ_P is the observed chemical shift and δ_P^Q and δ_P^C are the limit chemical shifts for free (K), and complexed (KS) kringle, respectively, and $[K_0] = [K] + [KS]$, is the total kringle 4 concentration. As derived elsewhere (De Marco et al. 1982) Eq. (2) can be expressed as follows

$$\Delta_P^{-1} = 1 + 1/K_a([S_0] - [K_0]\,\Delta_P)\ \text{corr} \qquad (3)$$

which, in turn, can be formulated to read

$$[S_0]\ \text{corr}\,(1/\Delta_P - 1) = [K_0]\,\text{corr}\,(1 - \Delta_P) + 1/K_a\,, \qquad (4)$$

where $[S_0]$ is the total ligand concentration if the volume were kept constant, and "corr" is a factor we now introduce, which applies to both $[K_0]$ and $[S_0]$, in order to correct for progressive dilution brought about by the successive ligand additions. Notice that throughout a ligand titration experiment $[K_0]$ is constant, being equal to the initial concentration of the kringle, while $[S_0]$ increases. A problem that arises is that $[K_0]$ is not known with sufficient accuracy.

While Eq. (3) is useful for deriving K_a, $[K_0]$ being a fixed parameter, a linear fit to Eq. (4) yields both $[K_0]$ and K_a values. The procedure we have followed is to use Eq. (4) to obtain an initial estimate of $[K_0]$, then introduce this value into Eq. (3) and systematically vary it until an optimal fit was reached as judged by r^2, the linear correlation coefficient squared, keeping in mind that the intercept (Eq. (3)) should be ~ 1 (Fig. 7). Results extracted from these analyses are listed in Table 2.

Useful information can also be derived from the dependence of the ligand chemical shift on the ligand concentration during complexation. In this analysis A and B in Eq. (1) would represent the free and kringle-complexed ligand states, respectively,

Table 2. Ligand-binding parameters from kringle 4 ligand titration experiments

	K_a $(\text{m}M^{-1})$ [a]	k_{off} (s^{-1}) [b]	k_{on} $(M^{-1}s^{-1})$ [c]
εACA	21 ± 1	$(5.3 \pm 0.3) \times 10^3$	$(1.1 \pm 0.1) \times 10^8$
AcLys	37 ± 1	$(4.0 \pm 0.2) \times 10^3$	$(1.5 \pm 0.1) \times 10^8$
AMCHA	159 ± 2	$(1.3 \pm 0.1) \times 10^3$	$(2.0 \pm 0.1) \times 10^8$
BASA	74 ± 2	$(0.8 \pm 0.0_2) \times 10^3$	$(0.6 \pm 0.0_3) \times 10^8$

[a] Data extracted from the linear fittings shown in Fig. 7
[b] Based on Eq. (11) and the curve fittings shown in Fig. 9
[c] Calculated: $k_{on} = K_a \cdot k_{off}$

while X would stand for the free kringle. In analogy to Eq. (2), we define

$$\Delta_L \equiv (\delta_L - \delta_L^Q)/(\delta_L^C - \delta_L^Q) = [KS]/[S_0] \qquad (5)$$

for the ligand resonances. Both Δ_P and Δ_L are related in that they depend on the molar fraction, or relative population, of the kringle-ligand complex. Since in our experiments we have titrated the protein with the ligand, at the start of the titrations the kringle was mostly unbound ($\Delta_P \sim 0$), while the free ligand level would be very low, the ligand being mostly bound, so that $\Delta_L \sim 1$. We notice that

$$\Delta_L/\Delta_P = [K_0]/[S_0] \qquad (6)$$

which can be formulated to read

$$[S_0]\,\Delta_L = C + [K_0]\,\Delta_P \qquad (7)$$

in order to perform a standard linear fitting, where the intercept C should result ~ 0. For this analysis AcLys provides a most informative ligand since the acyl CH_3 group affords a NMR probe which is

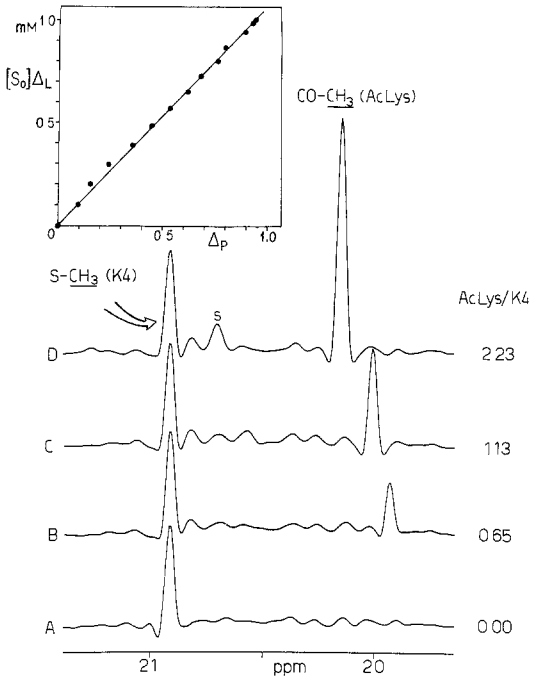

Fig. 8. Kringle 4 titration with AcLys: shifts of the ligand acyl methyl group resonance. An unaffected kringle 4 Met CH_3^{ε} resonance is manifest at ~2.09 ppm (Hochschwender et al. 1983); *S* denotes a spinning side band arising from the ligand acyl CH_3 singlet. The inset contains a linear fitting of AcLys titration data for kringle 4. The *straight line* is plotted according to Eq. (7), the *slope* in the linear fitting yields $[K_0]$. Δ_P represents an average over a number of kringle resonances, whereas Δ_L was obtained from the chemical shift of the ligand acyl CH_3 resonance. Spectra recorded at 600 MHz

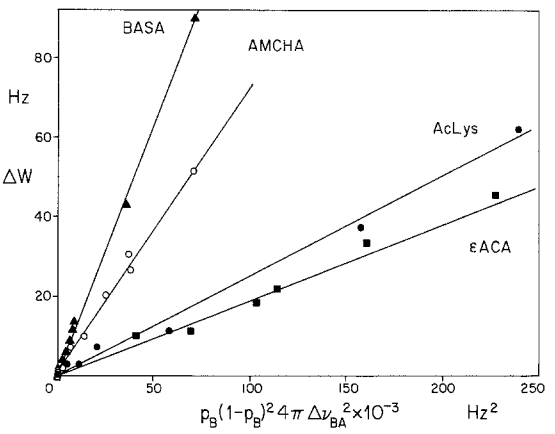

Fig. 9. Linear fitting of ligand titration data for kringle 4: BASA (▲), εACA (■), AcLys (●), and AMCHA (○). The *straight lines* are plotted according to Eq. (11), so that the *slopes* yield k_{off}^{-1} (see text)

measurably affected by kringle-binding (Fig. 8). For this ligand we obtaine $[K_0] = 1.05$ m*M* a value close to $[K_0] = 1.09$ m*M*, as estimated from fitting Eqs. (3) or (4). It should be noticed that

$$1 - \Delta_L = [S]/[S_0] \tag{8}$$

so that the expression for the Langmuir isotherm

$$[KS]^{-1} = [K_0]^{-1} + 1/K_a[K_0][S] \tag{9}$$

now becomes

$$\Delta_P = 1 + 1/K_a[S_0](1 - \Delta_L)\,\mathrm{corr} \tag{10}$$

which is a one-parameter fitting, formally identical to Eq. (3), when calculating K_a. From Eq. (9) one readily obtains K_a via a linear least squares fit. It is gratifying that, for AcLys, we derive $K_a = 37 \pm 1$ mM^{-1} by fitting either Eqs. (3), (4) or (10).

Ligand dissociation kinetics

The acyl CH_3 signal from AcLys remains consistently sharp throughout the whole ligand titration experiment (Fig. 8). On the other hand, the broad, ring current-shifted CH_2 resonances from AMCHA (Fig. 2) and from the other aliphatic ligands (Llinás et al. 1985; De Marco et al. 1986), often unsuitable for accurate chemical shift determinations, were found useful for estimating k_{off}.

As derived by Sudmeier et al. (1980), the excess broadening during complexation, ΔW, is given by

$$\Delta W = W - W_0 = 4\pi\Delta\nu_{BA}^2 p_B(1 - p_B)^2/k_{off}, \tag{11}$$

where, by reference to Eq. (1), p_A and p_B are the populations of states *A* and *B*, k_{off} (k_{on}) is the ligand-kringle dissociation (association) constant, and $\Delta\nu_{BA}$ is the chemical shift difference, in Hz, between the *B* and *A* states for a given resonance. Thus, if $\Delta\nu_{BA}$ is known, k_{off} can be derived on the basis of Eq. (11) by monitoring signals which are sufficiently resolved to yield reliable estimates of ΔW in the course of the ligand titration experiment.

The enhanced line broadening induced on some kringle 4 resonances upon substoichiometric BASA additions, makes this ligand a convenient one to derive a good estimate of k_{off} from protein resonances. In particular, the His^{33} H2 signal near 8.3 ppm (singlet 8) and the high-field Trp^{72} H2 resonance near 6.7 ppm (singlet 1) prove to be excellent probes (Hochschwender et al. 1983). Line widths were estimated from spectral simulations; p_B values resulted from an average Δ_P, determined from a set of non-broadened signals as exchange-broadening causes linearity between Δ_P and δ no longer to be fulfilled (Sudmeier et al. 1980). From fitting Eq. (11) for the two singlets (Fig. 9), we derive $k_{off} = 805$ s^{-1} ($r^2 = 0.99$).

With the aliphatic ligands, the signals which broaden appreciably during complexation are those from the ligands themselves, in particular those

from the CH_2 resonances shifted below 0 ppm (Fig. 2). In principle, the line width-chemical shift analysis of these resonances can be obscured by a number of problems:

a. The monitored signals are unresolved complex multiplets so that estimates of line width differences are not reliable.
b. The ligand CH_2 resonances, although well characterized for the free molecules, have not been specifically assigned in the complex so that $\Delta\nu_{BA}$ is not unequivocally determined.
c. ν_B is unknown.

Regarding point (a), the *original* line width and splittings of the multiplets are only marginally relevant, since we are interested only in the slope of our experimental ΔW while, in Eq. (11), W_0 affects only the intercept. Concerning point (b), since $p_B (= \Delta_L)$ is function of $\Delta\gamma_{BA}$, a sort of internal compensation affects Eq. (11) so that, within the experimental error, the $p_B(1-p_B)^2 4\pi\Delta\nu_{BA}^2$ values turn out to be fairly independent of a proper match between the broadened multiplets and the corresponding methylene (H^β, H^γ, H^δ etc.) resonances in the free ligand spectrum. In other words, if an assignment is reversed, e.g. by confusing H^β for H^ε, $\Delta\nu_{BA}^2$ will decrease, but $p_B(1-p_B)^2$ will increase and their product does not change significantly. This can be justified more rigorously: taking into account that $1-p_B = p_A = (\nu_B - \nu)/(\nu_B - \nu_A)$ and that $\Delta\nu_{BA} = (\nu_B - \nu_A)$, Eq. (11) can be written

$$\Delta W = \frac{4\pi}{k_{off}} \frac{(\nu - \nu_A)(\nu_B - \nu)^2}{(\nu_B - \nu_A)}$$

and, since initially the ligand is mostly all bound $\nu \sim \nu_B$ and $(\nu - \nu_A)/(\nu_B - \nu_A) \sim 1$ so that (11) becomes essentially independent of ν_A, hence of the correct assignment. Equation (11) remains, though, strongly dependent on ν_B, which leads to question c. For ν_B, it turns out that it is straightforward to derive its value graphically, by extrapolation.

For both the AcLys and εACA titrations (Fig. 9), we have resorted to analyze those resonances between 0 and − 1 ppm (Llinás et al. 1985; De Marco et al. 1986) which are sufficiently resolved to yield the most accurate chemical shift and line width data. For AMCHA, the excess line broadening values for the three resonances from the bound ligand which appear the furtherest high-field were used. These are the two one-proton peaks labelled a and b, and the two-proton peak labelled c and d, in Fig. 2. The best fit for (11) was obtained when all three peaks were taken as arising from equatorial ring protons. The results of these analyses are listed in Table 2, which also includes $k_{on} (= K_a \cdot k_{off})$ values.

Conclusions

The values for the association constants listed in Table 2 show significant differences in binding affinity to kringle 4 for the various ligands, with K_a ranging from 21 mM^{-1} for εACA to 159 mM^{-1} for AMCHA. The value for BASA, $K_a = 74\ mM^{-1}$, agrees with a preliminary estimate based on lesser quality titration data (Hochschwender et al. 1983). The data also indicate an almost 2-fold preference of kringle 4 towards AMCHA relative to BASA, which suggests that the higher conformational flexibility of the cyclohexyl ring might facilitate a fit at the binding site.

The aromatic nature of the BASA ring is expected to favor lipophilic interactions with other aromatics at the binding-site, the Trp^{72} indole group in particular (Llinás et al. 1983; Llinás et al. 1985; De Marco et al. 1986). This is consistent with the stronger affinity of kringle 4 toward BASA, vis á vis εACA and AcLys, despite the larger structural flexibility of the latter to adapt to the steric requirements of the ligand-binding site. One may also speculate that doubling the number of CH_2 groups at the β and γ positions in AMCHA, could lead to an increase in kringle-ligand contacts and thus to an enhanced intermolecular interaction as our study indicates a ~ 7.6-fold stronger binding of AMCHA relative to εACA. This agrees qualitatively with the studies of Winn et al. (1980), based on the displacement of kringle 4 from lysine-Sepharose by lysine analogs, which suggest a 4.35-fold preference towards AMCHA relative to εACA, and of Cole and Castellino (1984), based on measuring the ligand competition against a kringle 4 binding-site-specific monoclonal antibody, which indicate a 3.7-fold stronger binding for the cyclic ligand versus the linear one. Furthermore, our estimate for AMCHA, $K_a \sim 159\ mM^{-1}$, matches excellently the value $K_a \sim 158\ mM^{-1}$ determined for this ligand by Markus et al. (1981) via equilibrium ultrafiltration experiments at pH 8.0. Similarly, good agreement is manifested between our K_a value value for εACA, 21 mM^{-1}, and that reported by Lerch et al. (1980) 27.5 mM^{-1} based on equilibrium dialysis experiments at pH 7.4.

On the basis of the model Eq. (11), the k_{on} values we derive indicate that the ligand-binding kinetics is close to being diffusion-controlled suggesting a favorable entropy factor for the ligands to penetrate the lysine-binding site. It is interesting that, as expected from the bulkiness of the ligand, BASA exhibits the slowest insertion rate (smallest k_{on}). However, it still represents a tightly bound ligand (large K_a) simply because its k_{off} is also small. In contrast, AcLys (the closest analog to the

putative physiological ligand) seems to exhibit great facility to both penetrate and leave the ligand-binding site. Rather surprising is the large k_{on} of AMCHA, suggesting a structural feature of the molecule (probably its chair or boat conformations) that favours its insertion at the binding site. Clearly, a temperature-dependence study of K_a, k_{on} and k_{off} for the various ligands is mandatory in order to refine modelling the dynamics of ligand-kringle interaction. Such a study is in progress.

Acknowledgements. This project was supported by the U.S. Public Health Service, NIH grants HL 15535 and HL 29409. The 600 MHz NMR facility is supported by grant RR 00292 from the National Institutes of Health.

References

Bok RA, Mangel WF (1985) Quantitative characterization of the binding of plasminogen to intact fibrin clots. Biochemistry 24:3279–3286

Bundi A, Wüthrich K (1979) ^{1}H-NMR parameters of the common amino acid residues measured in aqueous solutions of the linear tetrapeptides H-Gly-Gly-X-L-Ala-OH. Biopolymers 18:285–297

Christensen U (1984) The AH-site of plasminogen and two C-terminal fragments. Biochem J 223:413–421

Cole KR, Castellino FJ (1984) The binding of antifibrinolytic amino acids to kringle 4-containing fragments of plasminogen. Arch Biochem Biophys 229:568–575

De Marco A (1977) pH dependence of internal references. J Magn Reson 26:527–528

De Marco A, Hochschwender SM, Laursen RA, Llinás M (1982) Human plasminogen: proton NMR studies on kringle 1. J Biol Chem 257:12716–12721

De Marco A, Laursen RA, Llinás M (1985a) Proton Overhauser experiments on kringle 4 from human plasminogen. Implications for the structure of the kringle's hydrophobic core. Biochim Biophys Acta 827:369–380

De Marco A, Pluck ND, Bányai L, Trexler M, Laursen RA, Patthy L, Llinás M, Williams RJP (1985b) Analysis and identification of aromatic signals in the proton magnetic resonance spectrum of the kringle 4 fragment from human plasminogen. Biochemistry 24:748–753

De Marco A, Laursen RA, Llinás M (1986) ^{1}H-NMR spectroscopic manifestions of ligand-binding to the kringle 4 domain of human plasminogen. Arch Biochem Biophys 244:727–741

Deutsch DG, Mertz ET (1970) Plasminogen: purification from human plasma by affinity chromatography. Science 170: 1095–1096

Feeney J, Batchelor JG, Albrand JP, Roberts GCK (1979) The effects of intermediate exchange processes on the estimation of equilibrium constants by NMR. J Magn Reson 33: 519–529

Hochschwender SM, Laursen RA, De Marco A, Llinás M (1983) 600 MHz ^{1}H-nuclear magnetic studies of the kringle 4 fragment of human plasminogen. Arch Biochem Biophys 223:58–67

Lerch PG, Rickli EE, Lergier W, Gillessen D (1980) Localization of individual lysine-binding regions in human plasminogen and investigations on their complex-forming properties. Eur J Biochem 107:7–13

Llinás M, De Marco A, Hochschwender SM, Laursen RA (1983) A ^{1}H-NMR study of isolated domains from human plasminogen: structural homology between kringles 1 and 4. Eur J Biochem 135:379–391

Llinás M, Motta A, De Marco A, Laursen RA (1985) Kringle 4 from human plasminogen: ^{1}H-NMR study of the interactions between ω-amino acid ligands and aromatic residues at the lysine-binding site. Proc Int Symp Biomol Struct Interact (Suppl J Biosci) 8:121–139

Lucas MA, Fretto LJ, McKee PD (1983) The binding of human plasminogen to fibrin and fibrinogen. J Biol Chem 258:4249–4256

Markus G, Camiolo SM, Sottrup-Jensen L, Magnusson S (1981) Tranexamic acid binding to kringle-containing fragments of human plasminogen. Progr Fibrinolysis 5: 125–128

Markwardt F (1978) Synthetic inhibitors of fibrinolysis. In: Markwardt F (ed) Fibrinolytics and antifibrinolytics. Springer, Berlin Heidelberg New York, pp 511–577

Okamoto S, Oshiba S, Mihara H, Okamoto U (1968) Synthetic inhibitors of fibrinolysis: in vitro and in vivo mode of action. Ann NY Acad Sci 146:414–429

Ramesh V, Gyenes M, Patthy L, Llinás M (1986) The aromatic ^{1}H-NMR spectrum of plasminogen kringle 4: a comparative study of human, porcine and bovine homologs. Eur J Biochem 159:581–595

Sottrup-Jensen L, Claeys H, Zajdel M, Petersen TE, Magnusson S (1978) The primary structure of human plasminogen: isolation of two lysine-binding fragments and one "mini"-plasminogen (MW, 38,000) by elastase-catalyzed-specific limited proteolysis. Progr Chem Fibrinolysis Thrombolysis 3:191–209

Sudmeier JL, Evelhoch JL, Jonsson NBH (1980) Dependence of NMR lineshape analysis upon chemical rates and mechanisms: implications for enzyme histidine titrations. J Magn Reson 40:377–390

Thorsen S, Clemmensen I, Sottrup-Jensen L, Magnusson S (1981) Adsorption to fibrin of native fragments of known primary structure from human plasminogen. Biochim Biophys Acta 668:377–387

Trexler M, Bányai L, Patthy L, Pluck ND, Williams RJP (1983) NMR studies on native and several chemically modified kringle 4 species of human plasminogen. FEBS Lett 154:311–318

Váli Z, Patthy L (1982) Location of the intermediate and high-affinity ω-aminocarboxylic acid-binding sites in human plasminogen. J Biol Chem 257:2104–2110

Váli Z, Patthy L (1984) The fibrin-binding site of human plasminogen: arginines 32 and 34 are essential for fibrin affinity of the kringle 1 domain. J Biol Chem 259:13690–13694

Wiman B, Collen D (1978) Molecular mechanism of physiological fibrinolysis. Nature 272:549–550

Winn ES, Hu SP, Hochschwender SM, Laursen RA (1980) Studies on the lysine-binding sites of human plasminogen: the effect of ligand structure on the binding of lysine analogs to plasminogen. Eur J Biochem 104:579–586